Study of the Reactions $O^{18}(p,n)F^{18}$, $O^{18}(p,p'\gamma)O^{18}$, and $O^{18}(p,\alpha_{1,2}\gamma)N^{15}$ from $E_p=2500$ to 3000 keV*

F. W. Prosser, Jr., G. U. Din,† and D. D. Tolbert
The University of Kansas, Lawrence, Kansas

(Received 7 October 1966)

The reactions $O^{18}(p,n)F^{18}$, $O^{18}(p,p'\gamma)O^{18}$, and $O^{18}(p,\alpha_{1,2}\gamma)N^{15}$ were investigated in the energy range $E_p=2500$ to 3000 keV by simultaneous observation of the neutrons, 1.98-MeV γ rays, and 5.30-MeV γ rays. Angular distributions of the 1.98-MeV γ rays were measured at the five prominent inelastic scattering resonances. The threshold for neutron production was found to be 2577±3 keV. The following resonances in the three decay channels were identified: (neutron) 2645, 2696, 2722, 2769, and 2926 keV; (alpha) 2645, 2769, and 2926 keV; and (proton) 2633, 2705, 2732, 2769, and 2926 keV. Spins and parities were assigned to several of these resonances: 2633, $\frac{5}{2}^{(+)}$; 2645, $(\frac{3}{2})$; 2705, $\frac{3}{2}^{(+)}$; 2732, $\frac{5}{2}^{(+)}(\frac{7}{2})$; and 2769, $\frac{5}{2}^{(+)}$. All parity assignments, as well as the spin assignment of the 2645-keV resonance, are based on physical arguments. Comparison of the properties of the elastic scattering resonance at 849 keV and the resonances at 2633 (and 2732) and 2705 keV with those of the known and theoretically predicted states in O^{19} indicates that they are isobaric-spin analog states; however, isobaric-spin impurities are present.

I. INTRODUCTION

A NUMBER of investigations of the particle reactions induced by the proton bombardment of O^{18} have been made. Hill and Blair,[1] in their study of the $O^{18}(p,n)F^{18}$ and $O^{18}(p,\alpha)N^{15}$ reactions from $E_p=0.08$ to 3.5 MeV, were the first to observe that several of the resonances occurring in the α-particle channel appeared to be shifted somewhat in energy from apparently corresponding resonances in the neutron channel. They suggested interference effects or the influence of large spin values as possible sources of this shift. Blair and Leigh,[2] in a later investigation of these same reactions, found that all resonances observed by them in the neutron channel had corresponding resonances in the α-particle channel, but that there were additional resonances in the latter which, at certain angles, caused structure to appear in the excitation curve resembling shifted resonances.

Carlson *et al.*[3] investigated the elastic scattering cross section as well as the $O^{18}(p,\alpha)N^{15}$ reaction over this same energy range using gas targets. They confirmed most of the results of Blair *et al.*[1,2] and found additional resonances. At proton energies above 2.75 MeV, they were able to observe the particle groups from inelastic scattering and from formation of N^{15} in its (unresolved) first and second excited states. Yagi *et al.*[4] have also measured the elastic scattering and $O^{18}(p,\alpha)N^{15}$ cross sections in the range from $E_p=0.6$ to 1.4 MeV, and Yagi[5] has assigned spins, parities, and partial widths to several resonances. Beard *et al.*[6] have made accurate measurements of the energies and widths of several resonances in the $O^{18}(p,n)F^{18}$ reaction using very thin gas targets. In addition, they have given the most precise value, 2576±1 keV, for the threshold of this reaction, based on the simultaneous measurement of neutron and proton energies.

In the present experiment we have measured the yield of neutrons, 1.98-MeV γ rays from inelastic scattering, and 5.30-MeV γ rays from the excited states of N^{15} to locate the resonances in these channels and to help eliminate some of the ambiguities which exist in the energies assigned to the resonances. To eliminate the effect of (real or apparent) energy shifts with angle of observation, excitation curves were obtained with the neutron and γ-ray detectors alternated among the angle 0°, 90°, and 155°. The angular distributions of the 1.98-MeV γ radiation were measured at the five resonances which appeared prominently in the inelastic channel. These angular distributions allowed spin and tentative parity assignments to be made for several of the resonances. In addition, the properties of two of these resonances were found to suggest strongly that they are the isobaric spin analogs to known states in O^{19}.

II. EXPERIMENTAL PROCEDURE

This work was carried out with the University of Kansas 3-MeV Van de Graaff accelerator. The proton beam was analyzed in the 25° beam deflecting magnet and its energy determined by the measurement of the magnetic field with a standard NMR device. The energy calibration was based on the measurement of the $Li^7(p,n)$ threshold, using the value 1880.36±0.22 keV,[7] and checked for consistency at the $Be^9(p,n)$ and $B^{11}(p,n)$ thresholds.

The neutron detector consisted of a 1 in. diam×1-mm-thick Li^6I scintillation crystal, with the crystal and photomultiplier tube enclosed in a Lucite cylinder with a minimum thickness of 2.5 cm and an outer diameter

* Supported in part by the U. S. Atomic Energy Commission.
† Now at the Australian National University, Canberra, Australia.
[1] H. A. Hill and J. M. Blair, Phys. Rev. **104**, 198 (1956).
[2] J. M. Blair and J. J. Leigh, Phys. Rev. **118**, 495 (1960).
[3] R. R. Carlson, C. C. Kim, J. A. Jacobs, and A. C. L. Barnard, Phys. Rev. **122**, 607 (1961).
[4] K. Yagi, K. Katori, H. Ohnuma, Y. Hashimoto, and Y. Nogami, J. Phys. Soc. Japan **17**, 595 (1962).
[5] K. Yagi, J. Phys. Soc. Japan **17**, 604 (1962).
[6] P. M. Beard, Jr., E. G. Bilpuch, and P. B. Parks, Bull. Am. Phys. Soc. **10**, 462 (1965); private communication.
[7] J. B. Marion, University of Maryland, Technical Report No. 320, 1963 (unpublished).

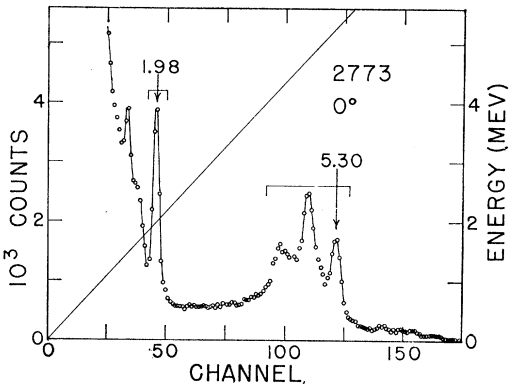

FIG. 1. Pulse-height spectrum obtained at $E_p=2773$ keV with the 3-in.×3-in. NaI detector. The detector was at 0° with respect to the beam. The full-energy peaks of the γ rays from the reactions $O^{18}(p,p'\gamma)O^{18}$ and $O^{18}(p,\alpha_{1,2}\gamma)N^{15}$ are indicated, together with the location of the single-channel windows used to obtain the excitation curves for these reactions. The background caused by neutrons can be seen to rise rapidly only below channel 40 and to be very small in the region of interest.

of 9.5 cm for moderation of the neutrons. The front face of the Lucite cylinder was 7 cm from the target. The pulse-height spectrum showed that the peak from thermal neutron detection was well removed from a continuum of small pulses resulting from γ-ray interaction with the crystal. Therefore, all pulses above a threshold set with an integral discriminator were counted.

A 3 in.×3 in. NaI crystal was used for the detection of the γ radiation. The front surface of the crystal was placed 25 cm from the target for the measurement of the excitation curve and 37 cm for the angular distributions. The output pulses from the photomultiplier tube, after amplification, were sorted in a 400-channel analyzer and in two single-channel analyzers. These had windows set to accept pulses corresponding to the full energy peak of the 1.98-MeV γ radiation and to the full energy and escape peaks of the 5.30-MeV γ radiation. These windows are indicated in the typical spectrum, obtained at $E_p=2773$ keV, shown in Fig. 1. The energy calibration curve shown was based on standard sources and reactions and the agreement of the structure appearing in the spectrum with its assigned energies is apparent, as is the clear separation of the 1.98-MeV full-energy peak from the neutron-induced background. For the excitation curves, the multichannel analyzer was used primarily to facilitate checking of the single-channel windows at frequent intervals; the recorded data were obtained from the scalers. For the angular distribution measurements, the yield of the 1.98-MeV γ radiation was determined by integration of the area under the full-energy peak in the spectrum after subtraction of the underlying Compton tails from higher-energy γ rays. This was accomplished by a least-squares fit of the full-energy peak to a Gaussian shape, which eliminated the effect of small gain changes encountered in the course of the experiment. A few runs for which the fitted width of the Gaussian varied significantly from the average value were discarded as unreliable.

The O^{18} target was prepared at Rice University by heating a tungsten disk, 0.75 in. diam × 0.02 in. thick, in an induction heater in an atmosphere of oxygen enriched to 90% in O^{18}. The target thickness was determined to be 8.6±0.6 keV from the 4.3±0.3-keV shift in apparent energy of the 2663- and 2645-keV resonances as the angle between the beam and the normal to the target was changed from 0° to 60°. For all other measurements the target was left perpendicular to the beam.

The target chamber was an aluminum cylinder lined with tantalum to suppress reactions initiated by scattered beam, with the target mounted at its axis. It was isolated from the deflecting magnet and the accelerator by two liquid-nitrogen cold traps which served to inhibit the deposition of carbon and other contaminants on the target surface. This was only partially successful, and the target was repositioned slightly at intervals to present a clean area to the beam. The presence and uncertain thickness of this carbon layer caused the principal uncertainty in the resonance and threshold energies.

A beam current of about one microampere was employed throughout this experiment. The collected charge was measured with an Elcor A309B current integrator. Each point on the excitation curves corresponds to a total charge of 100 μC, while the points on the first two and last three angular distributions were taken for 200 and 500 μC, respectively. The excitation curve was obtained at intervals of 10 kc/sec of the NMR frequency, an average of about 3 keV over the energy range covered, and repeated at intervals of 5 kc/sec in regions of interest. Many of these data were

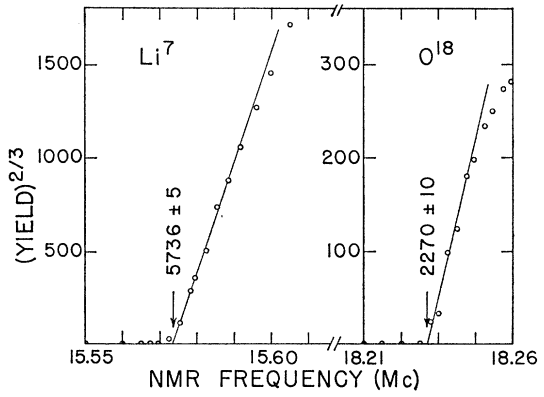

FIG. 2. Threshold measurements of the $O^{18}(p,n)F^{18}$ and $Li^7(p,n)Be^7$ reactions. The two-thirds power of the yield has been plotted to facilitate linear extrapolations to the true thresholds. The indicated threshold frequencies of 15.5736±0.0005 and 18.2270±0.0010 Mc/sec and the recommended value of 1880.36 ±0.22 keV (see Ref. 7) yield the value 2577±1 keV for the $O^{18}(p,n)F^{18}$ threshold. The assigned uncertainty of 3 keV given in the text is based on the reproducibility of this value.

rechecked at least once and in some cases twice over a period of two months and, in all cases, proved reproducible within statistics.

III. RESULTS

The data obtained at the $O^{18}(p,n)F^{18}$ threshold are shown in Fig. 2. The value obtained, 2577±3 keV, is in excellent agreement with that obtained by Beard *et al.*[6] As mentioned above, the principal source of uncertainty was the amount of carbon present on the target at the time of the measurement.

The excitation curves obtained for the three reactions are shown in Figs. 3–5. For the data shown in Fig. 3, the neutron counter was at 0° and the γ-ray counter at 90°; for those shown in Fig. 4, the two detectors were interchanged; and for those shown in Fig. 5, the two detectors were at back angles on opposite sides of the beam. The values obtained for the resonance energies and widths, both corrected for target thickness, are listed in Table I and compared with the values obtained by other investigators. Several features of interest appear in these excitation curves. First, it is clear that the inelastic scattering resonances at 2633, 2705, and 2732 keV are distinct from those appearing in the other channels at 2645, 2696, and 2722 keV. This displacement occurs at all three angles in a consistent manner and cannot, therefore, be a result of interference effects. The anomalous shape of the 2633-keV resonance in Fig. 3 results from the presence of the Compton tail from the 5.30-MeV radiation in the single-channel window set for the 1.98-MeV radiation and the relative weakness of the latter at this angle. The same effect occurs at the 2769-keV resonance where it causes an apparent strength of the inelastic scattering about 30% greater than the actual strength. The two higher resonances appear in all three channels at the same energy.

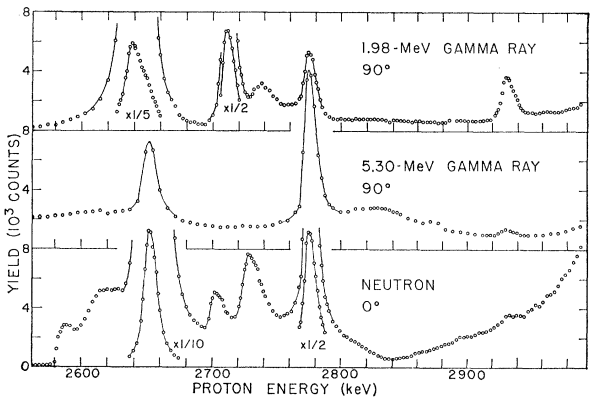

FIG. 3. Excitation curve for the reactions $O^{18}(p,n)F^{18}$, $O^{18}(p,\alpha_{1,2}\gamma)N^{15}$, and $O^{18}(p,p'\gamma)O^{18}$. For these data, the neutron detector was at 0° with respect to the beam and the γ-ray detector at 90°. The data represented are the counting rates (per 100 μC) of discriminators with windows set as described in the text and in Fig. 1. Room backgrounds taken with the beam stopped on a tantalum shutter 6 ft from the target have been subtracted.

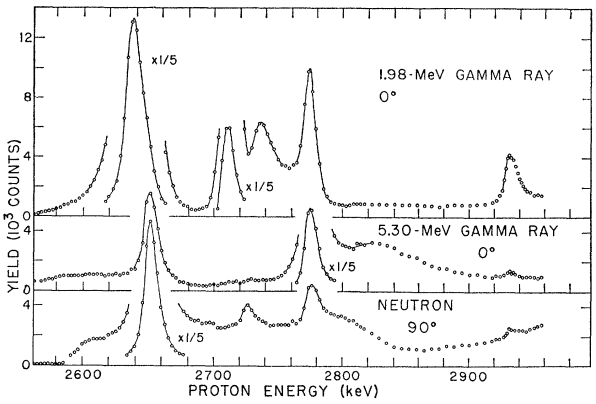

FIG. 4. Identical with Fig. 3, except the angles at which the detectors were placed have been interchanged.

Next a previously unreported neutron resonance has been found at 2696 keV in the present study and independently by Beard *et al.*[6] and the resonance at 2926 keV reported in several other reactions is observed to occur weakly also in the neutron channel. Finally, there appears to be a broad structure centered about 2.80 MeV in the neutron channel and another at about 2.83 MeV in the α-particle channel which are undoubtedly to be associated with the several resonances reported in this energy region by other observers.[1–4] The widths obtained in the present study, when corrected for the 8-keV target thickness, agree reasonably well with the other measurements of the widths reported.[1,6]

The large uncertainty in target composition precludes calculation of resonance strengths, $\omega\gamma$, with sufficient precision to justify their inclusion in Table I. However, an approximate scale factor will be useful in the discussion below and can be estimated on two bases. If the active layer is assumed to be pure WO_3, the strength of the 2633-keV resonance is $\omega\gamma=1.2$ keV. This is a reasonable upper limit for the oxygen concentration and therefore a lower limit on the resonance strength. Alternatively, Carlson *et al.* have measured differential cross sections for inelastic scattering, beginning with the 2769-keV resonance.[3] If the particle group is assumed to have an isotropic angular distribution, agreement between their results and those of the present investigation requires that the average oxygen concentration be about one-sixth of the above estimate and leads to a value of $\omega\gamma=4.5$ keV for the 2633-keV resonance. For comparison, the upper limit for $\omega\gamma$ is $\omega\Gamma_t/4$ or 11.3 keV for this resonance, with $J=\frac{5}{2}$ as discussed below.

The angular distributions of the 1.98-MeV γ radiation measured at the peaks of the five inelastic scattering resonances are shown in Fig. 6. The circles are the experimental data, corrected for absorption in the target backing. The solid lines are the least-squares fit to the expression $W(\theta)=A_0[1+A_2P_2(\cos\theta)+A_4P_4(\cos\theta)]$. The values obtained for the coefficients together with

TABLE I. Energy levels in F^{19} observed in proton-induced reactions on O^{18}. The excitation energy in F^{19} is based on the value 7.992 MeV for $O^{18}+p-F^{19}$.[a] The channels are labeled by the emerging particle, e.g., α' designates α-particle emission to the excited states of N^{15}. Resonance energies and widths are given in the laboratory system.

					Blair *et al.*[b]			Carlson *et al.*[c]		Beard *et al.*[d]	
E_x (MeV)	E_p(lab) (keV)	Γ(lab) (keV)	Channel	J^π	E_p(lab) (keV)	Γ(lab) (keV)	Channel	E_p(lab) (keV)	Channel	E_p(lab) (keV)	Γ(lab) (keV)
10.505	2633±3	15±2	p'	$\frac{5}{2}^{(+)}$	2635±5		α	2636±8	p, α		
10.517	2645±3	9±2	n, α	$(\frac{3}{2})$	2649±5	10±3	n, α	2648±8	p, α	2643	6.5
15.565	2696±4	12±4	n							2692	1.6
10.574	2705±3	8±2	p'	$\frac{3}{2}^{(+)}$	2712±5		α	2708±8	p, α		
10.590	2722±4	15±4	n		2726±5		n, α	2726±8	p, α	2717	5.5
10.600	2732±4	23±3	p'	$\frac{5}{2}^{(+)}(\frac{7}{2})$							
10.635	2769±3	7±3	n, p', α'	$\frac{5}{2}^{(+)}$	2772±5	<20	n, α	2768±8	p, α, p'	2767	5.0
								2800±8	p, α		
								2824±8	p, α		
10.785	2926±3	8±2	n, p', α'	$(\geq\frac{5}{2})$	2929±5		α	2926±8	p, α, p'		

[a] See Ref. 12.
[b] See Refs. 1 and 2.
[c] See Ref. 3. An evident error exists in Fig. 4 and Table I of this reference mislabeling the resonance at 2926 keV.
[d] See Ref. 6.

their standard deviations are listed in Table II, where the small corrections for finite solid angle have been made.[8]

IV. ANGULAR-MOMENTUM ASSIGNMENTS

Theoretical expressions for the angular correlations of $(a,b\gamma)$ reactions have been given by several authors. One particularly convenient for the case here of unobserved intermediate radiation is that of Sharp *et al.*[9] When specialized to the present experiment, where the entrance channel has a unique channel spin of $\frac{1}{2}$ and sharp angular momentum l determined by the spin and parity of the compound state and the observed γ radiation must be pure $E2$, their expression becomes

$$W(\theta_\gamma)=\sum(-)^{L_{12}-\frac{1}{2}}Z(lJlJ;\tfrac{1}{2}k)W(J2J2;L_{12}k)\times Z_1(2222;0k)P_k(\cos\theta_\gamma).$$

Here Z, W, and Z_1 are Racah and associated coefficients,[9] l and J are the entrance channel angular momentum and compound state spin, and L_{12} is the total angular momentum, $l'\pm\frac{1}{2}$, of the emitted particle. The Z coefficients in this case are independent of l for the two permitted values $J\pm\frac{1}{2}$; hence the distribution is determined entirely by J and L_{12}.

Further, L_{12} is restricted by the conditions $|J-2|\leq L_{12}\leq J+2$ and $L_{12}=l'\pm\frac{1}{2}$. The allowed values of L_{12} for a given J^π and the corresponding values of l' are shown in Table III. The range of L_{12} is seen to be independent of the parity of the compound state, a special case of the general theorem that parity cannot be determined by angular correlation measurements alone. However, the relatively low energy available in the inelastic channel may be expected to weigh heavily against contributions from higher values of l', particularly since mixing in L_{12}, and hence in l', is incoherent.

Because of the strict restriction of k to 0, 2, and 4, the experimental angular distributions and the theoretical predictions may be conveniently displayed on an A_2 versus A_4 graph. This has been done in Fig. 7. The experimentally determined angular distributions are represented by their error ellipses, i.e., the two-dimensional analogs to the standard deviation for a single variable. The error ellipses are based strictly on

TABLE II. Angular distributions of the 1.98-MeV γ radiation at the five inelastic scattering resonances. The coefficients were obtained in a least-squares fit of the integrated yield in the full energy peak to the expression $W(\theta)=A_0[1+A_2P_2(\cos\theta)+A_4P_4(\cos\theta)]$. A_2 and A_4 have been corrected for finite solid angle. The quoted errors are standard deviations.

Resonance energy (keV)	A_0 (counts/10^{-4} C)	A_2	A_4
2633	22 605±63	0.547±0.006	−0.556±0.006
2705	7182±41	0.486±0.012	−0.048±0.012
2732	1728± 9	0.522±0.011	−0.304±0.012
2769	2298±19	0.498±0.015	−0.490±0.017
2926	1352±17	0.070±0.024	−0.151±0.025

[8] A. L. Stanford, Jr., and W. K. Rivers, Jr., Rev. Sci. Instr. **30**, 719 (1959).
[9] W. T. Sharp, J. M. Kennedy, B. J. Sears, and M. G. Hoyle, Atomic Energy of Canada, Ltd., AECL-97, 1954 (unpublished).

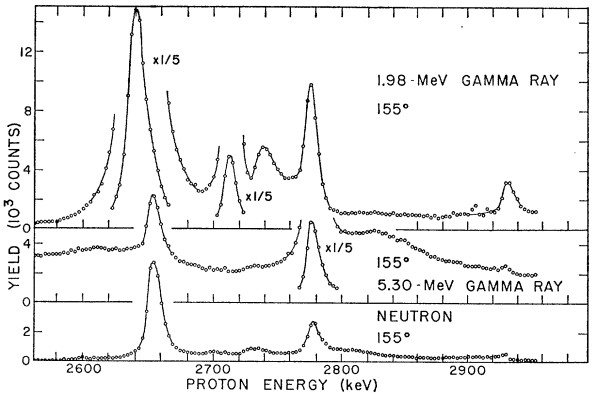

FIG. 5. Identical with Fig. 3, except the two detectors were at an angle of 155° with respect to the beam and on opposite sides of the beam.

TABLE III. Allowed values of orbital angular momentum l' for various spins and parities of the compound state.

J^π \ L_{12}	$\frac{1}{2}$	$\frac{3}{2}$	$\frac{5}{2}$	$\frac{7}{2}$	$\frac{9}{2}$	$\frac{11}{2}$
$\frac{3}{2}^+$	0	2	2	4		
$\frac{3}{2}^-$	1	1	3	3		
$\frac{5}{2}^+$	0	2	2	4	4	
$\frac{5}{2}^-$	1	1	3	3	5	
$\frac{7}{2}^+$		2	2	4	4	6
$\frac{7}{2}^-$		1	3	3	5	5

the statistical accuracy of the measurements; neither their size nor location include any attempt to correct for the effects of neighboring resonances or of possible nonresonant background. The theoretical predictions are labeled by $J^\pi(l')$. Thus the triangle formed by the point $\frac{5}{2}^+(0)$ and the line $\frac{5}{2}^+(2)$ contains all possibilities for a $\frac{5}{2}^+$ resonance if $l'=4$ may be ignored. *Clearly, unambiguous spin assignments can be made only under fortuitous circumstances.* However, when the information from such a diagram is combined with penetrability arguments and the presence or absence of competition in other channels, strong inferences about spins and parities can be made. The assignments that could be made in the present investigation will be discussed below and are summarized in Table I.

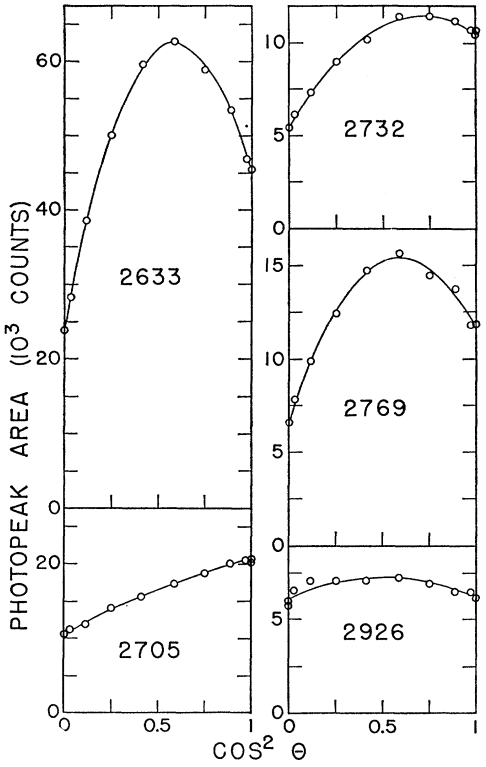

FIG. 6. Angular distributions of the 1.98-MeV γ radiations at the five inelastic scattering resonances. The circles are the experimental points, while the solid lines are the least-squares fit of a Legendre polynomial series to them. The standard deviations of the points are equal to or less than the size of the circles. The energies of the five resonances, in keV, are indicated for each distribution. Where repeated points, at 0° and 90°, differed by more than the sum of their standard deviations, both points are shown.

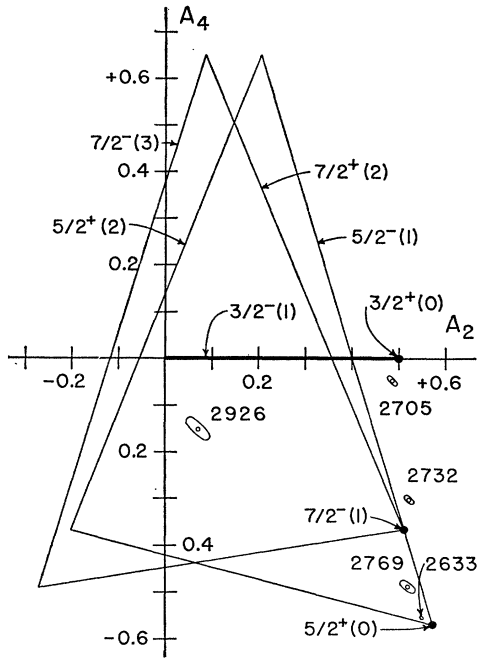

FIG. 7. A_2-versus-A_4 graph, showing the theoretically allowed and experimentally obtained angular distributions. The experimental angular distributions are shown as circles enclosed by their error ellipses, and they are labeled by the energy, in keV, of the resonance at which they were obtained. The theoretical distributions, labeled by $J^\pi(l')$, are represented by dots or lines for cases where one or two values of L_{12}, respectively, are allowed (see Table III). The two triangles represent the distributions which can occur for a $\frac{5}{2}^+$ and $\frac{7}{2}^-$ resonance under the restriction to the two lower values of l' allowed in each case.

A. The 2633-keV Resonance

The presence of the strongest inelastic scattering resonance in the region surveyed at the lowest energy (540 keV above threshold) is almost sufficient evidence to conclude that $l'=0$. Such a conclusion is further supported by the near agreement of the angular distribution with the $\frac{5}{2}^+(0)$ point (see Fig. 7). A $\frac{5}{2}^-$ assignment cannot be eliminated, but must be considered to be much less likely. The Wigner limits on the partial widths for $l'=0$ and 1 are 23 keV and 3.3 keV, respectively.[10] From the value $\omega\gamma=4.5$ keV as estimated above and the measured value Γ_t(c.m.)$=14$ keV, the inelastic width is either 1.7 or 12 keV. (The presence of some decay[3] to the ground state of N^{15} will tend to increase the smaller and decrease the larger of these

[10] The Wigner limit for $F^{19}\rightarrow O^{18}+p$ has been calculated from the expression $3(1\,\frac{1}{2}\,-1\,\frac{1}{2}|\,\tau\,\frac{1}{2})^2\hbar^2/2\mu R^2$, with $R=3.8\times10^{-13}$ cm. The squared Clebsch-Gordan coefficient has the values $\frac{2}{3}$ and $\frac{1}{3}$ for $\tau=\frac{1}{2}$ and $\frac{3}{2}$, respectively. For these estimates where τ is unknown, the average value $\frac{1}{2}$ has been used; in Sec. V, the appropriate value $\frac{1}{3}$ is used.

extremes.) Thus a negative parity assignment requires an inelastic width of greater than 50% of the Wigner limit, an unlikely value at this excitation energy. An additional argument in favor of a positive parity assignment is that a virtually pure value of $L_{12}=\frac{1}{2}$ is required by the observed angular distribution; as indicated in Table III, this value is strongly favored on the basis of penetrability for a $\frac{5}{2}^+$ assignment, whereas $L_{12}=\frac{3}{2}$ is equally probable for a $\frac{5}{2}^-$ assignment.

The small departure from a pure $\frac{5}{2}^+(0)$ angular distribution can be caused by several possible perturbations, e.g., the presence of small, undetected resonances or of a small amount of $l'=2$ inelastic scattering. However there is no evidence for the former and the latter cannot account for the entire discrepancy without violation of the Wigner limit. A third effect which must be present, and which may be expected to be unusually important in view of the relatively thick target backing used here, is small angle Compton scattering between source and detector. This scattering obviously will lead to a decrease in the observed anisotropy, but the magnitude of the effect is difficult to calculate since it depends not only on the scattering material present but also on the energy resolution of the detector.

B. The 2645-keV Resonance

This resonance occurs only 68 keV above the threshold for neutron emission and is the strongest in the neutron channel; hence it is likely that $l_n=0$ and $J^\pi=(\frac{1}{2},\frac{3}{2})^+$. The appearance of α emission to the $\frac{1}{2}^+$ and/or $\frac{5}{2}^+$ states in N^{15} and the apparent absence of inelastic scattering agree best with the choice $\frac{1}{2}^+$. However, the marked anisotropy[2,3] of the ground-state α group rules out this choice. The angular distribution of this group agrees qualitatively with a $\frac{3}{2}$ or $\frac{5}{2}$ assignment, but the importance of interference with nearby resonances prevents a simple choice between these on this basis. On the basis of the available information, the best choice is $\frac{3}{2}$, but $\frac{5}{2}^-$ cannot be completely ruled out.

C. The 2705-keV Resonance

Again the strength of the inelastic scattering suggests $l'=0$. The measured distribution lies close to the $\frac{3}{2}^+(0)$ point and, for the same reasons given in the discussion of the 2633-keV resonance, this is believed to be the best choice. The Wigner limit of about 10 keV[10] for $l'=1$ inelastic protons compared to the measured total width of 8 keV still renders the negative parity assignment unlikely. The presence of a small, but definite, $P_4(\cos\theta)$ term causes the measured distribution to fall in a region of the A_2-A_4 diagram inaccessible to the angular distribution from an isolated resonance. However, this can be explained by the presence of the tail of the 2633-keV resonance, of the nearby 2732-keV resonance (see below), and of possible weak underlying resonances not discernible in the yield curves. With an assignment of $\frac{3}{2}^+$, the absence of this resonance in the neutron channel and its near absence in the α-particle decay to the ground state of N^{15} which could occur with $l_\alpha=1$ need further explanation. (Blair *et al.*[1,2] and Carlson *et al.*[3] report only a very weak resonance in this latter channel at energies which appear to correspond to the 2705-keV resonance in this report.) The alternative $\frac{3}{2}^-$ possibility is little better since the neutron and inelastic proton channels still would permit equal orbital angular momenta and neutron emission would still be favored by a factor of twenty; hence the explanation must lie elsewhere. A possible interpretation of this will be discussed in Sec. V.

D. The 2732-keV Resonance

The angular distribution obtained for this weak resonance also falls into a region of Fig. 7 which is not accessible to an isolated resonance. Clearly this is a result of the (experimental or true) overlap with the 2705-keV resonance and possibly also with the 2769-keV resonance. Therefore the most probable assignment is $\frac{5}{2}$, although $\frac{7}{2}$ cannot be ruled out with certainty.

In an attempt to explain the anomalous features of the angular distributions at this and the 2705-keV resonances, the theoretical distributions were calculated assuming the measured resonance energies and widths and assignments of $\frac{5}{2}^+(0)$ and $\frac{3}{2}^+(0)$, respectively. In addition, the finite target thickness causes an increase in the incoherent contributions to the predicted distributions and this effect was included. The results were $W(\theta)=1+0.506P_2(\cos\theta)-0.049P_4(\cos\theta)$ and $1+0.552\times P_2(\cos\theta)-0.419P_4(\cos\theta)$ for the 2705- and 2732-keV resonances, respectively. Comparison with the measured values in Table II indicates satisfactory agreement, except for the value -0.419. However, this term is the most sensitive to the energy values used. For example, an increase by 2 keV in the assumed width of the 2705-keV resonance and a decrease of 2 keV in the separation of the resonances results in predictions of $1+0.506\times P_2(\cos\theta)-0.050P_4(\cos\theta)$ and $1+0.542P_2(\cos\theta)-0.333P_4(\cos\theta)$. These values are clearly in excellent agreement with the measured values, the remaining disagreement being of the same general type as that seen at the 2633-keV resonance. It should be noted that this interference occurs only if the resonances are of the same parity; the odd multipolarity terms characteristic of interference between different parity resonances vanish in this case because of the axial symmetry of the experiment and the sharp parity of the γ-ray emitting state.[11] Therefore, the parities of the 2705- and 2732-keV resonances, while not necessarily positive, are almost certainly the same.

E. The 2769-keV Resonance

This is the first resonance which is definitely present in all three channels. The measured angular distribution

[11] See, e.g., F. W. Prosser, Jr., in Proceedings of the Second Symposium on the Structure of Low-Medium Mass Nuclei, edited by P. Goldhammer and L. W. Seagondollar, 1966 (unpublished).

TABLE IV. Comparison of predicted $T=\frac{3}{2}$ states in F^{19} with several observed states. Excitation energies are based on 7.441 MeV calculated for the $T=\frac{3}{2}$ ground state and 7.992 MeV[a] for $O^{18}+p-F^{19}$. Experimental widths are given in the center-of-mass system. The predicted widths have been calculated at the energies of the states to which they are believed to correspond, with the channel radius taken to be 3.80×10^{-13} cm.

Predicted (experiment)[b]		Predicted (theory)[c]				Observed			
E_x (MeV)	J^π	E_x (MeV)	J^π	Γ_p (keV)	$\Gamma_{p'}$ (keV)	E_x (MeV)	J^π	Γ (keV)	E_p (keV)
7.441	$\frac{5}{2}^+$	7.441	$\frac{5}{2}^+$			7.43[d]			
7.537	$\frac{3}{2}^+$	7.482	$\frac{3}{2}^+$						
8.908	$\frac{1}{2}^+$	8.957	$\frac{1}{2}^+$	85		8.802	$\frac{1}{2}^+$	$25(\Gamma_p)$	849[e]
9.814	$(\frac{3}{2}^+,\frac{5}{2}^+,\frac{7}{2}^+)$[f]								
10.220	$\frac{9}{2}^+$	10.128	$\frac{9}{2}^+$						
10.511	$(\frac{3}{2}^+,\frac{5}{2}^+,\frac{7}{2}^+)$[f]	10.510	$\frac{3}{2}^+$		19.9	10.574	$\frac{3}{2}^+$	8	2705
10.597	$\frac{5}{2}^+$	10.558	$\frac{5}{2}^+$	4.2	9.3	10.505	$\frac{5}{2}^+$	14	2633
				4.6	21.1	10.600	$\frac{5}{2}(\frac{7}{2})$	22	2732
10.670	$\frac{1}{2}^+$								
		10.819	$\frac{7}{2}^+$						

[a] See Ref. 12. [b] See Ref. 16. [c] See Refs. 17 and 18. [d] See Ref. 14. [e] See Ref. 5. [f] See Ref. 15.

leads to a unique $J=\frac{5}{2}$ assignment. The parity assignment is rather more tenuous than those of the previous resonances desired, but a preference must be given to positive parity on the basis of relative penetrabilities and the proximity of the measured distributions to that of the pure $\frac{5}{2}^+$, $l'=0$ prediction.

F. The 2926-keV Resonance

This resonance is also present in all three channels, although only very weakly in the neutron and α-particle channels. The angular distribution, unlike the others, departs widely from any pure assignment, indicating either strong interference with neighboring resonances or the presence of abnormally large contributions from higher angular momenta in the inelastic channel. The $P_4(\cos\theta)$ term, if attributable to this resonance, requires that $J\geqslant\frac{5}{2}$. However, a comparison of the ratio of apparent yield of 1.98-MeV γ radiation in the excitation curves to that ratio at the other resonances indicates that there is a contribution to the angular distribution of about 20% from other sources. Since the anisotropy is small, it could arise in large measure from this source. Therefore, this lower limit on the angular momentum must be regarded as tentative.

V. ISOBARIC SPIN ASSIGNMENTS

A number of the compound states reached by proton interaction with O^{18} should be analogs to the low-lying states of O^{19}. The ground state of the $T=\frac{3}{2}$ system should occur at an excitation energy of 7.441 MeV in F^{19}, based on the $O^{17}-F^{17}$ mass difference[12] corrected for size effects[13] and the $O^{19}-F^{19}$ mass difference.[12] This agrees reasonably well with the state observed in the reaction $O^{18}(d,n\gamma)F^{19}$ at 7.43 ± 0.05 MeV and tentatively identified as the analog to the $\frac{5}{2}^+$ ground state of O^{19}.[14]

Recent measurements[15,16] and calculations[17,18] of the energies and characteristics of the lower states in O^{19} permit the prediction of the corresponding $T=\frac{3}{2}$ states in F^{19}. These predicted states, with their spins, are listed in Table IV.

The characteristic which may be expected to identify most clearly the $T=\frac{3}{2}$ states of F^{19} is an absence of decay through the neutron and α-particle channels which both require $T=\frac{1}{2}$. An evident example of this criterion is the 2705-keV resonance. Here decay through neither the neutron channel nor the α-particle channel is visible in the excitation curves shown in Figs. 3, 4, and 5, and the α-particle decay to the ground state of N^{15} is present but very weak.[3] Neither positive nor negative parity in conjunction with the $J=\frac{3}{2}$ assignment required by the angular distribution measurement of the 1.98-MeV γ rays can lead to the strong suppression of decay in these channels in preference to the inelastic channel. Further, the energy of this state is in reasonable agreement with the $J^\pi=\frac{3}{2}^+$, $T=\frac{3}{2}$ state to be expected in F^{19}, as indicated in Table IV. Hence, this lends credence to the $\frac{3}{2}^+$ assignment proposed above and it is proposed that this state is the analog to the 3.061-MeV state[15,16] in O^{19}.

If this assignment is correct, then the analog to the $J^\pi=\frac{5}{2}^+$ state at 3.153 MeV in O^{19} should be present about 90 keV higher in excitation. This agrees best in energy with the state at $E_p=2769$ keV and the most probable assignment, $J^\pi=\frac{5}{2}^+$, is also in agreement with such an identification. However, the strength of the neutron and α-particle channels relative to the inelastic scattering channel clearly argue against a $T=\frac{3}{2}$ assignment for this state.

[12] F. Everling, L. A. Konig, J. H. E. Mattauch, and A. H. Wapstra, Nucl. Phys. **15**, 342 (1960).
[13] D. H. Wilkinson, Phil. Mag. **1**, 1031 (1956).
[14] J. W. Butler, L. W. Fagg, and H. D. Holmgren, Phys. Rev. **113**, 268 (1959).
[15] R. Moreh, Nucl. Phys. **70**, 293 (1965).
[16] L. Wiza and R. Middleton, Phys. Rev. **143**, 676 (1966).
[17] R. D. Lawson (private communication).
[18] S. Cohen, R. D. Lawson, M. H. Macfarlane, and M. Soga, Phys. Letters **9**, 180 (1964).

Another possibility for such a state is the resonance at $E_p=2732$ keV. In the present investigation, it occurs only in the inelastic channel and the angular distribution is not incompatible with a $\frac{5}{2}^+$ assignment. If, however, the resonance reported in Refs. 2 and 3 at $E_p=2726$ keV should be identified with this resonance, rather than with the 2722-keV resonance as indicated in Table I, then a strong decay to the ground state of N^{15} is present at this resonance. In view of this possibility and the uncertainty of its spin assignment, no definite conclusion can realistically be reached.

The very strong inelastic scattering resonance at $E_p=2633$ keV is a third possibility for the $\frac{5}{2}^+$, $T=\frac{3}{2}$ state. As discussed above, it has a definite $J=\frac{5}{2}$ assignment with probable positive parity and it does not occur in the neutron channel nor in decay to the excited states of N^{15}. If it is the resonance reported at $E_p=2636$ in Ref. 3, it also decays to the ground state of N^{15} but with lower intensity than the resonances reported at $E_p=2726$ and 2768 keV.[3] Since the region of excitation covered in this investigation lies within the range where isobaric spin is expected to be least conserved,[19] mixing with nearby states with predominantly $T=\frac{1}{2}$ would explain this partial violation of the selection rules. Such states could well be those at $E_p=2732$ and/or 2769 keV.

The partial widths for elastic and inelastic scattering were calculated on the basis of the O^{18} and O^{19} wave functions of Lawson *et al.*[17,18] and the assumption that the 2705-keV and either the 2633- or 2732-keV resonances are, respectively, the expected $\frac{3}{2}^+$ and $\frac{5}{2}^+$ analog states and they are given in Table IV. The agreement with the experimental total widths is seen to be reasonably good, with a tendency for the predicted widths to be larger than the observed widths. Also, the elastic width for the $\frac{3}{2}^+$ state vanishes since only $d_{5/2}$ and $s_{1/2}$ orbitals are used in their wave functions. The calculations in O^{18} by Brown and Kuo[20] and in O^{18} and F^{19} by Inoue *et al.*[21] indicate that configurations with $d_{3/2}$ orbitals may be expected with amplitudes in the order of 10%. One would therefore expect a smaller, but nonzero elastic width for the $\frac{3}{2}^+$ state, as well as some reduction in the other calculated widths. This latter follows from the fact that the amplitudes of the configurations used would be correspondingly reduced and that there were no strong cancellations between matrix elements in the present calculations, a situation unlikely to continue as more terms are included.

The relative strength of the 2633-keV resonance must result not only from the near absence of decay in competing channels, but also from the near equality of elastic and inelastic widths. This agrees well with the predicted widths and tends to cause some preference for the identification of that resonance rather than the 2732-keV resonance as the $T=\frac{3}{2}$ state. On this same basis, the strength of the $\frac{3}{2}^+$ state is expected to be smaller both from the $2J+1$ statistical factor and the greater disparity between elastic and inelastic widths.

The strong elastic scattering resonance at $E_p=849$ keV, with $J^\pi=\frac{1}{2}^+$,[5] occurs at an excitation energy in reasonable agreement with that for the predicted $\frac{1}{2}^+$, $T=\frac{3}{2}$ state, as indicated in Table IV. As was the case at the higher resonances, the width calculated from the wave functions of Lawson *et al.*[17,18] disagrees with the measured elastic width by being too large. Here again decay to the ground state of N^{15} is present,[5] which clearly indicates the presence of considerable isobaric spin mixing. The properties of the neighboring broad resonance at $E_p=640$ keV [5] identify it as the principal source of $T=\frac{1}{2}$ contamination and thus support the inference that the upper state is primarily the analog to the $\frac{1}{2}^+$, 1.468-MeV state in O^{19}.

VI. SUMMARY

Evidence has been presented that identifies the resonances at $E_p=849$, 2633 (and 2732), and 2705 keV as the analog states to those in O^{19} at 1.467, 3.156, and 3.070 MeV,[14] respectively, in spite of the presence of isobaric spin impurity in the compound states. This identification, in turn, implies that the 3.070-MeV state in O^{19}, presently believed to have $J^\pi=\frac{3}{2}^+$, $\frac{5}{2}^+$, or $\frac{7}{2}^+$,[15] is the $\frac{3}{2}^+$ state predicted to be at 3.069 MeV.[17,18] The main basis of the argument has been the absence or relative weakness of the decay of those states in competing channels permitted or even favored by angular momentum selection rules. As can be seen from Table IV, this technique will not in general be available for the identification of the missing analog states in this region of F^{19}. With the exception of the $\frac{1}{2}^+$ state expected at about $E_x=10.670$ MeV, the formation of these states may be expected to be strongly inhibited in all particle channels and to appear strongly, if at all, only in the capture reaction. If this is the case, only the agreement in predicted spin and energy will serve to identify them.

ACKNOWLEDGMENTS

The authors gratefully acknowledge many helpful discussions with Professor Paul Goldhammer, and the assistance afforded by Dr. R. D. Lawson.

[19] D. H. Wilkinson, Phil. Mag. **1**, 379 (1956).
[20] T. T. S. Kuo and G. E. Brown, Nucl. Phys. **85**, 40 (1966).
[21] T. Inoue, T. Sebe, H. Hagiwara, and A. Arima, Nucl. Phys. **59**, 1 (1964).